EXAFS Study of Iron(III) Complexes of Sugar-type Ligands

L. NAGY*, H. OHTAKI

Department of Electronic Chemistry, Tokyo Institute of Technology, Nagatsuta, Midori-ku, Yokohama 227, Japan

T. YAMAGUCHI**

Department of Chemistry, Faculty of Science, Fukuoka University, Nanakuma, Jonan-ku, Fukuoka 814-01, Japan

and M. NOMURA

National Laboratory for High Energy Physics, Oho-machi, Tsukuba-gun, Ibaraki 305, Japan

(Received September 24, 1987; revised October 29, 1987)

Abstract

Three kinds of iron(III) complexes formed with sugar-type ligands, ketose, polyalcohol and sugar acid, were prepared. The Fe *K*-edge absorption spectra of the complexes were measured both in aqueous solution and in the solid state to reveal the structure from the analysis of their EXAFS and XANES. It was concluded that the iron(III) sugar complexes have a distorted octahedral structure with a mean Fe–O distance of 195 pm irrespective of the sugar type ligands both in aqueous solution and in the solid state. In the case of iron(III) fructose complex the dimerization of the complex was evidenced and the most likely structure was proposed.

Introduction

Although it has been known for about 100 years that sugars and sugar-type compounds can form complexes with metal ions, the field of sugar–metal complexes is still largely unexplored [1, 2]. For example, at least 70 crystalline complexes containing sugar and metal ions have been reported since 1973; the metal ions in these complexes are mainly those of group IA and IIA and most of their structures remain unknown. The literature on the complexation of sugar with transition metals has appeared in much more recent years and is less abundant. It is obvious that metal–sugar complexes play an important biological role in the transport phenomena of vital metal ions across cell membranes [3]. Recently, one of the authors (L.N.) and his coworkers studied complexation reactions between different transition metal ions and sugar-type compounds using various methods [4, 5] and a series of iron(III) complexes formed with aldoses, ketoses, polyalcohols, sugar acids, di- and trisaccharides were prepared [6]. It has been shown that deprotonated alcoholic hydroxy groups participate in the complex formation and polynuclear species are formed. Mössbauer spectra reflected the presence of high-spin iron(III) ions as the central atoms. EPR spectra showed antiferromagnetic interactions between the iron(III) centres in the complexes indicating the formation of dimeric or oligomeric complex structure.

In recent years EXAFS (Extended X-ray Absorption Fine Structure) spectroscopy has been proved to be successful in elucidating the short-range order of atoms in solution [7–9]. From the EXAFS method structural information can be obtained related to the radial distribution of atom pairs in a system; the number of neighbouring atom around a central atom (coordination number), the interatomic distance between them and its root-mean squares deviation. Our aim is, therefore, to determine the local structure of the sugar complexes of iron(III) ion in solution and in the solid state by the EXAFS method. XANES (X-ray Absorption Near Edge Structure) spectra of the sample solutions were also measured in order to obtain information on the electronic state of the iron atoms in the samples.

Experimental

Sample Preparations

Iron(III) perchlorate was prepared in the following way: iron(III) oxide was dissolved in concentrated hydrochloric acid. The iron(III) chloride thus formed was recrystallized from concentrated perchloric acid until no chloride ion was detected and was dried in a vacuum oven at 100 °C for two days.

The 10 mol dm^{-3} sodium hydroxide solution was purified according to D'ans and Mattner [10].

Sodium gluconate (Merck), D-fructose and mannitol were of Reanal products.

*Present address: Department of Inorganic and Analytical Chemistry, A. József University, H-6701 Szeged, P.O. Box 440, Hungary.

**Author to whom correspondence should be addressed.

0020-1693/89/$3.50

TABLE I. Samples Used for EXAFS Measurements in Aqueous Solution (aq) and in the Solid State (pw)

	Ligand (L)		(C_L/C_{Fe})[a]	pH[a]	Composition	C_{Fe} (mol dm^{-3})
A	Mannitol	aq	8	14		0.25
B	Mannitol	pw	8	14	$Fe_2L_2(OH)_2(H_2O)_4Na$	
C	Fructose	aq	2.5	11		0.17
D	Fructose	pw	2.5	11	$Fe_2L_2(OH)_2(H_2O)_4Na$	
E	Gluconate	aq	2.5	11		0.42
F	Gluconate	pw	2.5	11	$Fe_2L_2(OH)_4(H_2O)_2Na_2$	
G	Water[b]	pw			$FeNO_3 \cdot 9H_2O$	
H	Fe foil[b]					

[a] The values in initial solutions. [b] Structure standard.

The iron(III)–sugar complexes were prepared according to two basic prescriptions presented in refs. 6 and 11. Suitable portions of the aqueous solutions of iron(III) perchlorate and ligand were mixed to obtain a required ligand-to-metal molar ratio in the mixture. On the addition of sodium hydroxide to the solution, first the iron(III)–sugar complexes precipitated (this precipitate is probably a neutral complex [12], which is predominant at about pH = 3.5), which dissolved, however, with increasing pH of the solution. The pH change of the reaction mixture was controlled potentiometrically.

The iron(III)–sugar complexes were precipitated from their aqueous solutions by the addition of ethanol to make the final concentration of ethanol 80 vol./vol.%. The precipitate formed was collected by centrifugation and was redissolved in a small volume of water, the pH was adjusted again to be about 3.5, and to the resulting clear solution ethanol was added until the final concentration of ethanol was 80 vol./vol.%. The precipitate formed was collected again by centrifugation and successively washed with ethanol, acetone and ether, and was finally dried over P_2O_5.

The composition of the complexes was determined by the standard microanalytical method. The iron(III) content was determined by titration with EDTA; the sodium content was measured by atomic absorption spectroscopy. The results obtained for complexes prepared for the EXAFS analysis are in good agreement, within 4%, with the data published previously [6].

Samples measured by the EXAFS method were aqueous solutions containing iron(III)–mannitol, –D-fructose and –gluconato complexes. Solid samples of the same complexes were also measured for comparison. A crystalline powder of $Fe(NO_3)_3 \cdot 9H_2O$ containing hexaaqua iron(III) ions and iron foil were measured as the structure standards. Details of the samples are summarized in Table 1. All measurements were carried out at room temperature.

EXAFS Measurements

EXAFS and XANES spectra were measured around the Fe *K*-edge (7.11 keV) in transmission mode using BL10B station at the Photon Factory in the National Laboratory for High Energy Physics [13, 14]. A broad band synchrotron radiation is monochromatized by an Si(311) channel-cut crystal and passes through a sample placed between the first and the second ionization chambers, which were filled with N_2 and N_2(85%)+Ar(15%) gas, respectively.

Data Reduction Procedure

The EXAFS data were analysed by the following procedure: background absorption other than that for the *K*-edge of an absorption atom of interest was evaluated by a least-squares fitting procedure with Victorren's formulae [15] including a constant term to the pre-edge and was subtracted from the total absorption by extrapolation. The smooth *K*-shell absorption μ_0 due to an isolated atom was estimated by using a cubic spline function [16]. Two or three knots over the whole region were enough to give a good approximation for μ_0.

The modulation $\chi(k)$ was extracted and normalized by the following equation

$$\chi(k) = \{\mu(k) - \mu_0(k)\}/\mu_0(k) \quad (1)$$

where k is the photoelectron wave number of ejected electrons and is given as $\sqrt{2m(E-E_0)/\hbar^2}$. E denotes the energy of the incident X-rays and E_0 is the threshold energy for liberation of the photoelectron wave. In the present study, E_0 was selected as the position of the half height of the edge jump in all cases.

The resulting EXAFS modulation weighed with k^3 was Fourier transformed to give a radial distribution function, $\Phi(r)$.

Least-squares Calculations

The structural parameters (interatomic distance, r_j, mean-square displacement, σ_j^2, and coordination number, n_j) were obtained by comparing the observed EXAFS spectra and the model function given by the single scattering theory [17, 18] as

$$\chi(k)_{calc} = \Sigma\{n_j/(kr_j^2)\} \exp(-2\sigma_j^2 k^2) \exp(-2r_j/\lambda_j) F_j(\pi,k) \sin(2kr_j + \alpha_j(k)) \quad (2)$$

where $F_j(\pi,k)$ is the backscattering amplitude from each of n_j scatterers j at distance r_j from the X-ray absorbing atom. An amplitude reduction related to inelastic losses at the absorbing atom due to the many-body effect is introduced by the mean free path λ_j. $\alpha_j(k)$ is the total scattering phase shift experienced by the photoelectron.

The observed spectra can be compared with the theoretical ones by a least-squares fitting procedure in either r or k space. The latter procedure needs an additional Fourier backfiltering of the peak of interest in the $\Phi(r)$ curve. Theoretically, both analyses in the k or r space should give equivalent results. In the present study, we performed least-squares calculations in the k space, which were applied to the Fourier filtered k^3 weighted $\chi(k)_{obs}$ values to minimize the error-square sum U

$$U = \sum_{k_{min}}^{k_{max}} k^6\{\chi(k)_{obs} - \chi(k)_{calc}\}^2 \quad (3)$$

The values of $F_j(\pi,k)$ and $\alpha_j(k)$ in eqn. (2) were quoted from the tables reported by Teo and Lee [19]. The values are given against the absolute k values and thus an improper evaluation of E_0 should result in a systematic distortion of the k scale and affects the interatomic distances to be determined. Furthermore, the theoretical values of the back-scattering amplitudes $F_j(\pi,k)$ are usually larger by *ca.* 50% than those observed [19], which sometimes give unreasonable bond lengths between an X-ray absorbing central atom and its neighbouring ones and the coordination numbers. In the present study, λ_j was estimated from the standard samples of known structure and then used as constant in the course of the analysis of the EXAFS spectra of unknown samples, while $E_{0,j}$, r_j, σ_j and n_j were allowed to vary. Without detailed knowledge and evaluations of the immediate electronic environment of an absorbing atom, the value of the threshold energy is not known so that $E_{0,j}$ was also allowed to vary.

Results and Discussion

Figure 1 shows XANES spectra in the Fe K-edge region of reference compounds and of iron(III)–sugar complexes measured in solution and in the solid state. All spectra show a pre-edge peak attributable to the $1s \rightarrow 3d$ transition, the shape and intensity of which are typical for an octahedral coordination of iron(III) [20]. In the case of $Fe(NO_3)_3 \cdot 9H_2O$ crystals, which contain an octahedral $[Fe(H_2O)_6]^{3+}$ moiety [21], the spectrum exhibits a considerably sharp peak just above the absorption edge, which is accompanied by a weak shoulder structure as previously found [20] (Fig. 1G). The corresponding peak above the absorption edge of iron(III) sugar complexes is less sharp,

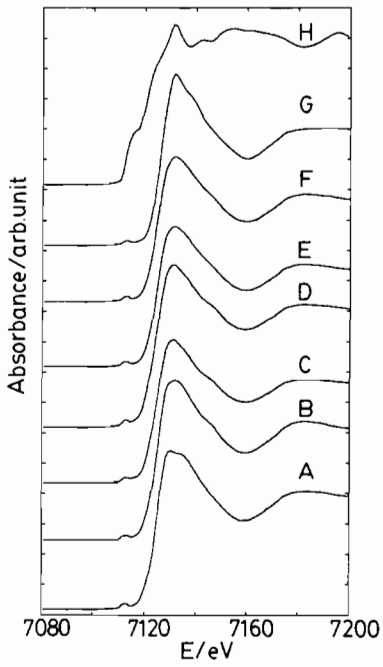

Fig. 1 XANES spectra of Fe(III)–mannitol (A: aq and B: pw), –fructose (C: aq and D: pw), –gluconato complexes (E: aq and F: pw), $FeNO_3 \cdot 9H_2O$ (G) and Fe foil (H).

compared with that of the iron(III) hydrate. It may be an indication of distorted octahedral Fe–O bondings resulting in a splitting of degenerate energy levels of iron(III) atom in the sugar complexes.

Prior to the EXAFS analysis for iron(III)–sugar complexes, we examined the spectra of $Fe(NO_3)_3 \cdot 9H_2O$ crystalline powder and iron foil as structure standard in order to estimate an effective value of λ_j.

In the crystal structure of $Fe(NO_3)_3 \cdot 9H_2O$ there are two crystallographically different $[Fe(H_2O)_6]^{3+}$ octahedra with a mean Fe(III)–O distance of 198.6 pm [21]. Figures 2G and 3G show, respectively, the observed k^3 weighted $\chi(k)$ values and the Fourier transform $\Phi(r)$ obtained over the k range of 0.03–0.115 pm^{-1}. The distinct peak at 160 pm in the $\Phi(r)$ (uncorrected for the phase shift) is certainly due to Fe–O bonds within the hexaaqua iron(III) ion. The k^3 weighted $\chi(k)$ spectrum of the first neighbour Fe–O interactions within the hexaaqua iron(III) ion was extracted by inverse Fourier transform of $\Phi(r)$ over the r range of 65–195 pm (Fig. 4G, dots).

Figures 2H and 3H show, respectively, the k^3 weighted $\chi(k)$ and $\Phi(r)$ values of iron foil. The k range used in the Fourier transform was 0.03–0.12 pm^{-1}. In the bcc form of iron metal eight Fe atoms are situated in the first-neighbour [22]. The distinct peak at 218 pm in the $\Phi(r)$ curve (Fig. 3H) corresponds to the first neighbour Fe–Fe interactions. The peaks at 353, 443 and 545 pm correspond to Fe atoms in outer shells. The contribution of the first

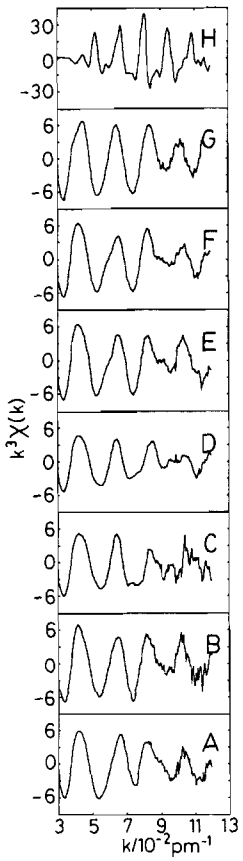

Fig. 2. k^3 weighted EXAFS pattern $\chi(k)$ of Fe(III)–mannitol (A: aq and B: pw), –fructose (C: aq and D: pw), –gluconato complexes (E: aq and F: pw), $FeNO_3 \cdot 9H_2O$ (G) and Fe foil (H).

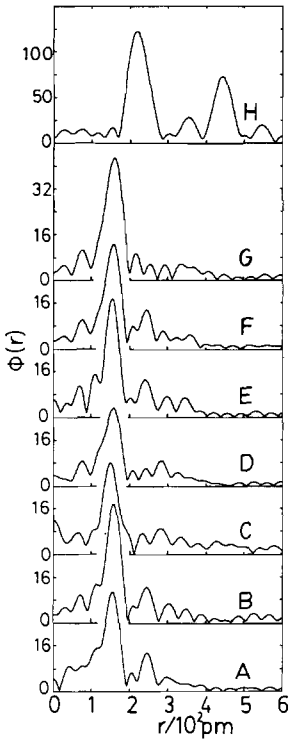

Fig. 3. Fourier transforms $\Phi(r)$ obtained from k^3 weighted $\chi(k)$ values in Fig. 2 (uncorrected for the phase shifts).

neighbour Fe–Fe interactions in the k space was obtained by Fourier filtering of the $\Phi(r)$ over the r range of 170–290 pm.

In the subsequent least-squares fits for the extracted k^3 weighted $\chi(k)$ values of the first neighbour interactions obtained above, $E_{0,j}$, r_j, λ_j and σ_j were allowed to vary simultaneously, while the coordination number was fixed at a known value (six and eight for the Fe–O and Fe–Fe pairs, respectively). The results of the curve-fitting analysis are given in Table 2. The Fe–O and Fe–Fe distances obtained from the present EXAFS analysis are in good agreement with crystallographic data.

The k^3 weighted $\chi(k)$ curves and Fourier transforms $\Phi(r)$ of iron(III)–sugar complexes in solution and in amorphous powder are depicted in Fig. 2A–F and 3A–F, respectively. In all cases, the k range transformed was 0.030–0.12 pm^{-1}.

For each sugar complex, the $\Phi(r)$ values obtained in aqueous solution are very similar to those of powder samples, and thus the iron(III)–sugar complex may have an analogous short-range structure in both states. The Fourier transform of each iron(III)–

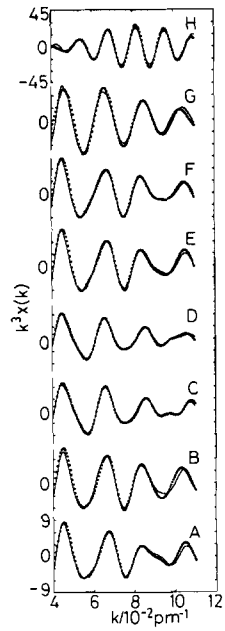

Fig. 4. A comparison between the Fourier filtered (dots) and fitted (solid lines) k^3 weighted $\chi(k)$ values of Fe(III)–mannitol (A: aq and B: pw), –fructose (C: aq and D: pw), –gluconato complexes (E: aq and F: pw), $FeNO_3 \cdot 9H_2O$ (G), and Fe foil (H).

TABLE 2. Results of the Curve-fitting Analysis for the Iron(III) Sugar Complexes in Aqueous Solution (aq) and in the Solid State (pw). The Values in Parentheses are X-ray Crystallographic Data. r, σ and n Represent the Interatomic Distance, the Root Mean Squares Displacement and the Coordination Number, Respectively

Ligand		Fe–O			Fe···C			Fe···Fe		
		r (pm)	σ (pm)	n	r (pm)	σ (pm)	n	r (pm)	σ (pm)	n
A Mannitol	aq	194	9.4	6.5	287	5.5	2.6			
B Mannitol	pw	198	7.3	6.1	285	5.0	2.2			
C Fructose	aq	192	9.8	6.0	277	6.9	2[b]	310	6.9	0.5
D Fructose	pw	194	10.1	5.7	285	9.3	2[b]	304	9.3	0.7
E Gluconate	aq	195	8.3	6.3	285	5.2	2.4			
F Gluconate	pw	196	8.7	6.3	283	5.0	2.3			
G Water	pw	196 190[c] (198.6[a])	8.7	6[b]						
H Fe foil								249 (249.2[d])	6.88	8[b]

[a]Ref. 21. [b]Fixed. [c]EXAFS result in ref. 20. [d]Ref. 22.

sugar complex has a similar feature; the sharp first peak around 160 pm and the second peak in the r range of 240–300 pm (uncorrected for the phase shift). It should be noted that in the case of the iron(III)–fructose complex the second peak splitted into two at 240 and 280 pm, compared with those for the other two sugar complexes.

The main peak at 160 pm in the $\Phi(r)$s (Fig. 3A–F) is assignable to Fe–O interactions within iron(III)–sugar complexes as expected from the $\Phi(r)$ of the iron(III) aqua complex (Fig. 3G). In order to estimate the first neighbour interactions in a quantitative manner, we extracted the corresponding EXAFS modulation by applying a window function (65 pm $\leqslant r \leqslant$ 205 pm) to the $\Phi(r)$ values, followed by Fourier transform to the k space (Fig. 4A–F). The Fourier filtered EXAFS modulation was then fitted to calculated values by means of a non-linear least-squares method with a constant empirical parameter λ_0 determined from the iron(III) hydrate system. The results of the preliminary fits showed that all iron(III)–sugar complexes have the coordination number close to six and the Fe–O distance expected for an octahedral coordination of iron(III) ion. This is consistent with the feature of the XANES spectra as previously discussed.

The peaks observed in the r range 240–300 pm in the $\Phi(r)$s of iron(III)–sugar complexes arise from the second nearest-neighbour atoms. One of the possible atoms present in the second neighbour should be carbon atoms connected to oxygen atoms bound to iron(III) ion as expected from the coordination geometry of sugar ligands around the iron(III) ion. When polymerization occurred via hydroxide oxygen bridges of iron(III)–sugar complexes as discussed in EPR measurements [6], Fe···Fe separations would also fall within a similar r range to Fe···C distances.

From the above considerations multi-shell fits were performed for k^3 weighted $\chi(k)$ Fourier filtered over 0.90–310 pm^{-1} in the following manner.

(1) Predominant first neighbour Fe–O interactions were expressed in terms of parameters $E_{0,O}$, r_O, σ_O and n_O, which were allowed to vary. λ_O was estimated from the data of crystalline iron(III) nitrate.

As to the second neighbour atoms the following three models were examined.

(2a) Only carbon atoms are present and no dimerization occurs.

(2b) Fe···Fe interactions are a predominant contributor to the peak and Fe···C pairs are negligible.

(2c) Both Fe···C and Fe···Fe interactions are responsible for the peak.

In each case $E_{0,j}$, r_j, σ_j and n_j were taken as independent variables. The value of λ_C was assumed to be the same as λ_O, while λ_{Fe} was determined from the data of iron foil.

The k range used in the fits was 0.04–0.11 pm^{-1}. According to the results of the fits, models (2a) and (2b) gave almost similar error squares sum U. The U value of model (2c) was slightly smaller, probably due to more parameters involved in the fits. In the three cases both Fe···C and Fe···Fe distances converged to 270–290 pm. These values are acceptable as Fe···C distances according to the literature of chelated compounds of iron(III).

The structure determination of crystalline compounds containing a dimeric $[Fe_2(OH)_2]^{4+}$ moiety is very few and only a single crystal X-ray study of di-μ-hydroxo-bis[2,6-pyridine-dicarboxylatoaquairon(III)] and di-μ-hydroxo-bis[4-hydroxo-2,6-pyridine-carboxylatoaquairon(III)] [23] has been reported by Thich *et al.* [23]. In both structures the $[Fe_2(OH)_2]^{4+}$ unit has a planar structure with Fe···Fe separation 307.8–308.9 pm, larger by 20–30 pm than the above

converged values (270–290 pm). This difference is beyond uncertainties* in the present EXAFS analysis. Thus, we concluded that the second peak of the iron(III)–mannitol complex originated mainly from Fe···C interactions.

In the case of the iron(III)–fructose complex, the second peak splitted into two at 240 and 280 pm, corresponding to the values 270 and 310 pm, respectively, after the phase shift correction either of carbon or of iron backscatter. The distance 310 pm is close to the literature value of the Fe···Fe interactions as noted above. The peak at 280 pm in the $\Phi(r)$ curve was thus attributed to Fe···Fe interactions, while that at 240 pm to Fe···C interactions. Although dimerization or polymerization was suggested also for iron(III)–mannitol and –gluconato complexes from Mössbauer and ESR studies [6], there might be no detectable amount of the dimer formed in the present mannitol and gluconato complexes by the EXAFS method.

The final results are summarized in Table 2. In Fig. 4 the Fourier filtered k^3 weighted $\chi(k)$ were reproduced well by the theoretical ones calculated with the values given in Table 2.

The average Fe–O distance within the iron(III)–sugar complexes is 195 pm irrespective of the sugar ligands. The value of 195 pm is consistent with the literature values for octahedral oxygen coordination of iron(III). The fact that the coordination number of iron(III) is six may lead, together with the indication from the XANES spectra, to a conclusion of a distorted octahedral arrangement of oxygen atoms around the central iron(III) ion.

Summarizing the experimental results obtained from the measurement of Fe K edge EXAFS and XANES, together with those found in earlier works for the same complexes by means of Mössbauer and ESR [6], we can propose a model structure of a binuclear iron(III) sugar complex as shown in Fig. 5. Two deprotonated alcoholic oxygen atoms (in the case of gluconato complex one alcoholic and one carboxylate oxygen atoms) coordinate to the iron(III) ion centre. Two free coordination sites of the iron(III) ion may be occupied by hydroxide ions, which form bridges between the two iron(III) ions. In all the complexes, iron(III) ion has the coordination

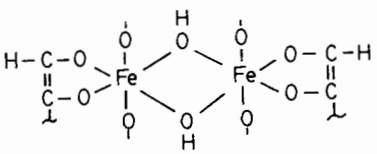

Fig. 5. The most likely structure of the binuclear Fe(III)–sugar complex.

*Uncertainties in interatomic distances are ±2 pm for the first shell and ±5 pm for outer shells. The errors in the coordination number is *ca.* ±0.5 atoms.

number of six. Consequently, two oxygen atoms either of OH^- ions or of sugar OH groups should be coordinated to fill the rest of the coordination sites of iron(III) ions forming an elongated octahedral arrangement.

According to ref. 23, the distance between the Fe atoms and bridged oxygen atoms falls within 193.8–199.3 pm. Thus, Fe–O(hydroxide ion) and Fe–O-(sugar ligand) bond lengths may be indistinguishable from the uncertainties of the EXAFS analysis. The Fe···Fe distance of 310 pm obtained in the present study is in good agreement with the value found in ref. 23.

The present EXAFS study has demonstrated the structure of polynuclear iron(III) complexes of sugar-type ligands suggested by previous Mössbauer and ESR measurements [6].

Supplementary Material

Tables of the raw absorption data, the observed and Fourier-filtered $k^3\chi(k)$ data and the Fourier transforms are available upon request to the author (T.Y.).

Acknowledgements

One of us (L.N.) would like to thank the Ministry of Education, Science and Culture of Japan and UNESCO for providing his financial support. This work has been performed under the approval of the Photon Factory Program Advisory Committee (Proposal No. 85-021). The present work is financially supported, in part, by the Ministry of Education, Science and Culture (Grant-in-Aid for Scientific Research on Priotity Area of Macromolecular Complex, No. 62612005).

References

1 J. A. Rendleman, Jr., *Adv. Carbohydr. Chem., 21* (1966) 209.
2 S. J. Angyal, *Pure Appl. Chem., 35* (1973) 131.
3 P. Saltman, *J. Chem. Educ., 42* (1965) 682.
4 L. Nagy, I. Horvath and K. Burger, *Inorg. Chim. Acta, 107* (1985) 179.
5 L. Nagy, T. Gajda, K. Burger and T. Pali, *Inorg. Chim. Acta, 123* (1986) 35.
6 L. Nagy, K. Burger, J. Kurti, M. A. Mustofa, L. Korecz and J. Kirisci, *Inorg. Chim. Acta, 124* (1986) 55.
7 D. R. Sandstrom, B. R. Stubbs and R. B. Greegar, Structural evidence for solutions from EXAFS measurements, in B. K. Teo and D. C. Joy (eds.), *EXAFS Spectroscopy*, Plenum, New York, 1981, Ch. 9, pp. 139–157.
8 T. Yamaguchi, O. Lindqvist, J. B. Boyce and T. Claeson, in K. O. Hodgson, B. Hedman and J. E. Pennen-Hahn (eds.), *EXAFS and Near Edge Structure III*, Springer, Berlin, 1984, pp. 417–419.
9 M. Sano, T. Maruo and H. Yamatera, *Bull. Chem. Soc. Jpn., 57* (1984) 275.
10 J. D'Ans and J. Mattner, *Angew. Chem., 64* (1952) 488.

11 P. J. Charley, B. Sarkar, C. F. Stitt and P. Saltman, *Biochim. Biophys. Acta, 69* (1963) 313.
12 B. Sarkar, P. Saltman, S. Benson and A. Adamson, *J. Inorg. Nucl. Chem., 26* (1964) 1551.
13 H. Oyanagi, T. Matsushita, M. Ito and H. Kuroda, *KEK Report 83-30,* National Laboratory for High Energy Physics, Oho-machi, Tsukuba 305, Japan, 1984.
14 M. Nomura, *KEK Report 85-7,* National Laboratory for High Energy Physics, Oho-machi, Tsukuba 305, Japan, 1985.
15 *International Tables for X-Ray Crystallography,* Vol. III, Kynoch Press, Birmingham, 1962, p. 161.
16 P. A. Lee, P. H. Citrin, P. Eisenberger and B. M. Kincaid, *Rev. Mod. Phys., 53* (1981) 769.
17 E. A. Stern, *Phys. Rev., B10* (1974) 3027.
18 B. Lengeler and P. Eisenberger, *Phys. Rev., B21* (1980) 4507.
19 B. K. Teo and P. A. Lee, *J. Am. Chem. Soc., 101* (1980) 2815.
20 K. Asakura, M. Nomura and H. Kuroda, *Bull. Chem. Soc. Jpn., 58* (1985) 1543.
21 N. J. Hair and J. K. Beattie, *Inorg. Chem., 16* (1977) 245.
22 *International Tables for X-Ray Crystallography,* Vol. III, Kynoch Press, Birmingham, 1962, p. 281.
23 J. A. Thich, C. C. Ou, D. Powers, B. Vasiliou, D. Mastropaolo, J. A. Potenza and H. J. Schugar, *J. Am. Chem. Soc., 98* (1976) 1425.